

## FREQUENCY SCANNING ANTENNA ARRAYS WITH METAMATERIAL BASED PHASED SHIFTERS

Nikola Bošković<sup>1</sup>, Branka Jokanović<sup>1</sup>, Vera Marković<sup>2</sup>

<sup>1</sup>Institute of Physics, University of Belgrade, Serbia

<sup>2</sup>Faculty of Electronic Engineering, University of Niš, Serbia

**Abstract.** *This paper presents a simple design of linear series-fed frequency scanning antenna arrays with: (a) identical rectangular dipoles and (b) pentagonal dipoles having different impedances to provide enhanced side lobe suppression. Phase shifters are designed as a metamaterial unit cell consisting of split-ring resonators coupled with the parallel microstrip line. Shifter models variations are described and control of phase is demonstrated. Two antenna arrays are manufactured and measured.*

**Key words:** *scanning antenna array, linear array, series feeding, pentagonal dipole, phase shifter, split-ring resonator.*

### 1. INTRODUCTION

Antenna elements come in various forms in terms of technology, size, cost and radiation properties. Nevertheless, a single antenna has a typical omnidirectional radiation pattern and low gain. In many applications, there is a need for directional and high gain radiation, which can be generated by combining multiple antenna elements in different arrangements. One of the most notable problems in antenna arrays is side lobe emergence. They can be observed as radiation in the unwanted direction as a direct consequence of the configuration of arrays elements. High levels of side lobes can make it hard to isolate desired signals and overcome uncertainties in the determination of a position of the specific object, which is especially important in radar applications. Two main factors, which determine the sidelobe levels (SLLs), are the power distribution between the elements and the distance between them. Typical demands are SLLs -20 dB [1], relative to the main lobe. SLLs from -30 to -20 dB can be typically achieved solely by the power distribution, but for higher lobes suppression, the distance between the elements must be considered as well.

Printed antennas are by far the most popular antennas for applications due to size and shape diversity, ease of fabrication and integration, low cost and high flexibility in resonant frequency, polarization, radiation pattern and impedance. They come in forms of patch,

---

Received November 2, 2018; received in revised form February 6, 2019

**Corresponding author:** Nikola Bošković

Institute of Physics, University of Belgrade, Pregrevica 118, 11080 Belgrade, Serbia

(E-mail: [nikolab@ipb.ac.rs](mailto:nikolab@ipb.ac.rs))

dipoles, slots etc. Their main drawback is a typical low power handling capability due to the low thermal conductivity of regularly used dielectrics. However, developing various dielectrics with high thermal conductivity similar to aluminum nitride (AlN) ceramic can overcome even this obstacle. Other problems like surface waves, spurious radiation and losses can be controlled in different ways [2-10].

In order to achieve low SLLs in frequency scanning antenna with linear element arrangements, the appropriate power distribution can be extremely hard to implement because it can require a very high ratio of the impedances of radiation elements. In addition, there is a need to maintain the desired distribution in a wide frequency band while avoiding main beam deformation, which can be caused by beam squinting due to the frequency change [11].

In this paper, experimental results from the array with regular dipoles comparing with the experimental results with the enhanced pentagonal dipoles are shown. Both models use the same shifter based on the four SRR, same dielectric, the distance between elements, and both are design to work at 10 GHz making it very fairly to use in comparison.

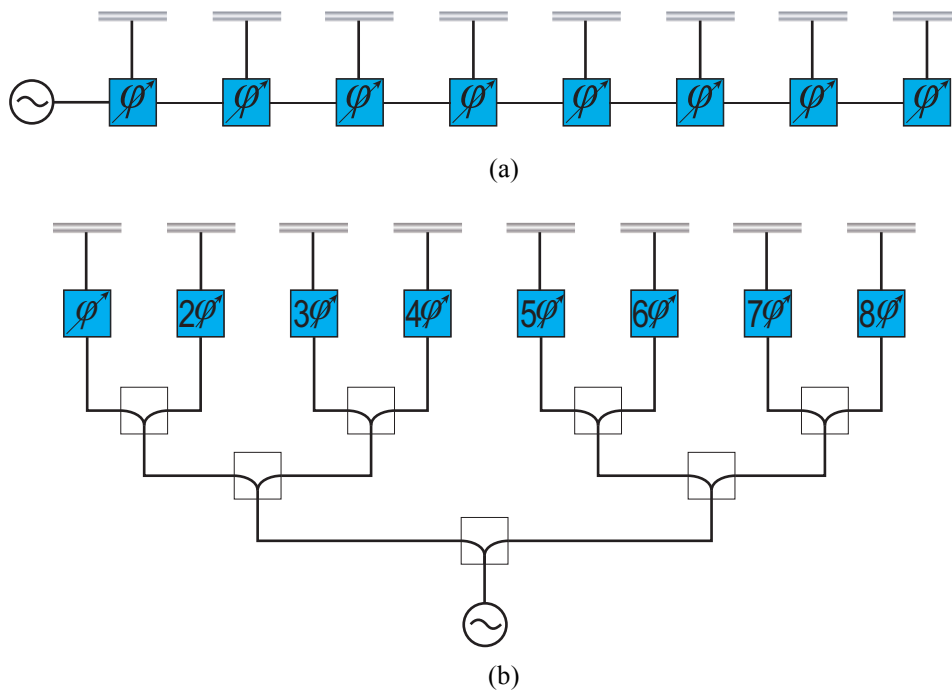


**Fig. 1** Antenna array feeds: (a) Series feed and (b) Corporate feed.

## 2. PRINTED FREQUENCY SCANNING ANTENNA

With technological development, there is a great need for the scanning antennas, which enable tracking of a specific position in space with great accuracy and resolution [12-15]. In the past, such solutions were predominantly based on a combination of the antenna array and a customized mechanical system for pointing the array at the specific direction. Such systems have limited agility, require periodic maintenance of the mechanical parts, and due to high price have limited usage. With the development of modern electronics, frequency scanning is introduced at a much lower price, better performances and reliability. Basic frequency scanning antenna array consists of the radiating elements in a specific spatial distribution and frequency dependent elements between them, which introduce different phase shift, depending on the applied frequency, hence this elements can be called phase shifters. A typical configuration is a linear series-fed array, which enables scanning in one plane. Combining multiple linear arrays in a planar array, we can obtain scanning in the second plane. Scanning in the second plane is typically achieved in a different manner than in a linear array.

Frequency scanning antenna enables continuous coverage of the spatial range of scanning. Angular resolution depends on the 3 dB-beamwidth of the main beam, and speed of scanning is determined by the frequency dependence of the phase shifter. For linear arrangements, an array of  $N$  radiating elements require  $N-1$  phase shifters, since for the basic operation phase shift  $\Delta\phi$  between two successive elements is constant, but there is also need for constant phase-increment from the first to the last element in the plane of scanning. Depending on their structure phase shifters can have significant losses and non-linearity, which can seriously degrade array characteristics. In addition, in order to provide low SLLs the suitable power distribution needs to be implemented, which can be challenging in a series-fed array (Fig 1a) because phase shifters and radiating elements change their performances in the frequency range. Because of that, full corporate-fed (Fig. 1b) are occasionally used, but they require a much greater number of phase shifters, have significantly larger size and smaller efficiency.

Other type of commonly used electronic scanning is via switchers. The principle is that every antenna element is connected to the power source via one of the several available phase shifters. With on/off switching shifter selection is made and the main beam is positioned at the certain direction. The whole system can work in a single frequency, but the number of available directions depends on the number of the phase shifts available. Similar basic principles of operations are used with Rotman lens [16-17], Butler matrix [18-19] and similar structures. They typically have  $N$  inputs and  $N$  outputs, which are connected to the antenna elements. When connecting the power source at the different inputs the different main beam positions are generated. Combining one of these types of electronic scanning in one plane and frequency scanning in another, scanning in two planes is enabled at the same time.

Frequency scanning antenna should be cheaper, easier to manufacture, with more stable characteristics in the working range, with higher efficiency and easier for integration with other components in comparison with the electronic scanning antenna. A natural choice would be a printed antenna structure with antenna elements having stable radiation and impedance characteristics in the working range. The printed pentagonal dipole is an excellent choice as a radiating element that satisfies demands for higher impedance bandwidth due to working at the second resonance and has stable radiation characteristics in the wide frequency band [20-21].

### 2.1. Antenna array technology

The printed dipole can be naturally implemented in two different technologies. One is coplanar stripline (CPS) and the other is symmetrical (balanced) microstrip line. CPS is a balanced uniplanar transmission line, consisting of two metallic conductor strips separated by a certain gap width, on a substrate. The CPS line is without bottom metallization of the substrate for the ground; instead, the virtual ground is placed at the symmetry plane between two conductors. The balanced microstrip line is equivalent to the classical microstrip line and is represented by two identical parallel transmission lines, one from each side of the dielectric surface. For the given substrate height and line width, the impedance of the balanced microstrip line would be equal to double the impedance of the microstrip line having identical width and half of the substrate height.

The CPS line offers flexibility in the design of planar microwave and millimeter-wave circuits, especially in mounting the solid-state device in series or shunt without via holes. It exhibits low loss, small dispersion, small discontinuity parasitics, considerable insensitivity to substrate thickness and simple implementation of open- and short- circuits. The CPS line has a typical impedance value around 200 Ohms, which is much higher than the typical microstrip line of 50 Ohms. In the series-fed array, it is very important to have available a high impedance ratio of the feeding transmission line and the radiating elements for achieving proper power distribution. Since the balanced microstrip line can achieve much lower impedance value, it is a better choice for this type of array.

### 2.2. Frequency scanning performance

The frequency bandwidth is a valuable and limited resource, and certain bands are restricted for specific use [22]. Two important parameters for frequency scanning systems are range and angular resolution. The angular resolution of beam scanning systems is defined by the antenna main lobe 3 dB beamwidth. It means that two identical targets at the same distance are resolved in angle if they are separated by more than the antenna 3 dB beamwidth. Antenna system with fixed beam provides only range resolution. Range resolution is the ability of an antenna system to distinguish between two or more targets on the same bearing but at different ranges. The pulse width is the primary factor in range resolution and it is generally the inverse of the pulse bandwidth. For the higher bandwidth available, the greater range precision can be obtained. Frequency scanning provides the angular resolution. Narrower 3 dB beamwidth provides greater precision in determining the angular position of the target. Frequency scanning systems performance is a typical trade-off between angular and range resolution.

The simplest phase shifter is a basic transmission line. Its length is directly proportional to phase shift contribution. Any phase shifter can be approximated with the transmission line of the certain length. Two parameters, which determine overall position of the main beam during scanning for the simple antenna array, are the distance between radiating elements ( $D$ ) and length of the transmission line ( $L$ ), as shown in Fig. 2.

Dependence between scanning angle  $\theta$  and relative frequency change  $\Delta f/f_0$  is given as:

$$\sin \theta = \frac{L}{2D} \left( \frac{\Delta f}{f_0} \right) = \frac{\Delta \phi}{360^\circ} \frac{\lambda_0}{D}, \quad \Delta f = f - f_0 \quad (1)$$

where the beam is steered over the limits  $\pm\theta$ ,  $f_0$  represent the central frequency at which the main beam is positioned broadside,  $\lambda_0$  is the free space length at the central frequency and  $\Delta\phi$  is the phase shift between two succeeding radiating elements (phase-increment). If the distance between the elements is fixed at the typical value of the  $0.5 \lambda_0$  (wavelength in free space at center frequency), the length  $L$  and the available frequency bandwidth will determine scanning properties.

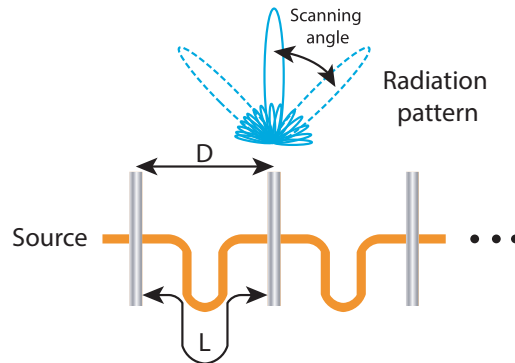


**Fig. 2** Frequency scanning antenna array with different positions of the main beam.

As can be seen, the same results for the scanning angle (sector) can be obtained independently for different values of  $L$  and  $\Delta f$ , while one of them is fixed. In practical application, frequency bandwidth is specified and  $L$  is used for obtaining a specific scanning angle. For the practical example, let us say that available relative bandwidth is 20% and required scanning is  $\pm 25^\circ$ , then from (1)  $L$  would have to be around  $4.2 D$ , that is  $2.1\lambda_0$  for the previously stated typical value of  $D$ . For 10% relative bandwidth, that value would be  $4.2\lambda_0$ . In both cases, the resulting phase shift would be around  $\pm 76$  degrees. Relative bandwidth in (1) would be equal to  $\Delta f / f_0$ , since total scanning sector is  $2\theta$ . From this, we can see that frequency sensitivity of the phased array is directly proportional to the equivalent length of the phase shifter.

### 2.3. Phase shifter performances

Transmission line although simple, typically has a very slow phase contribution with frequency change. For narrow bandwidth and large phase shift, it has to have substantial length. Long transmission lines can have significant losses and give rise to spurious radiation. If placed in the same plane as radiating elements, interaction might occur through the coupling and severe degradation of the radiation pattern could happen. For these reasons often other structures are employed as the phase shifter, which are better suited for the specific purpose.

In Fig. 3a it is shown phase shifter based on the metamaterial *left-handed* cell consisting of the pair of SRRs (split ring resonators) in balanced microstrip technology, where one metal layer is on top and the second identical at the bottom side of the dielectric. In microstrip, it would be single SRR cell coupled with transmission line with via in center in order to provide pass-band characteristics. Such shifter is used in [23], where it enabled scanning sector of  $32^\circ$  in 5% of the relative bandwidth. If we applied that as an angle  $\theta = \pm 16^\circ$  in (1), we can see that phase shift would be around  $\pm 50$  degrees and required  $L$

would be around  $5.5\lambda_0$ . Such a long line would take significant space and would require special care in order to minimize its impact on the radiation elements. The substrate used in [23] is Rogers 4003C with the dielectric constant of 3.55, height of 1 mm, loss tangent is 0.0027. Surface roughness in Rogers 4003C is 2.8 microns.

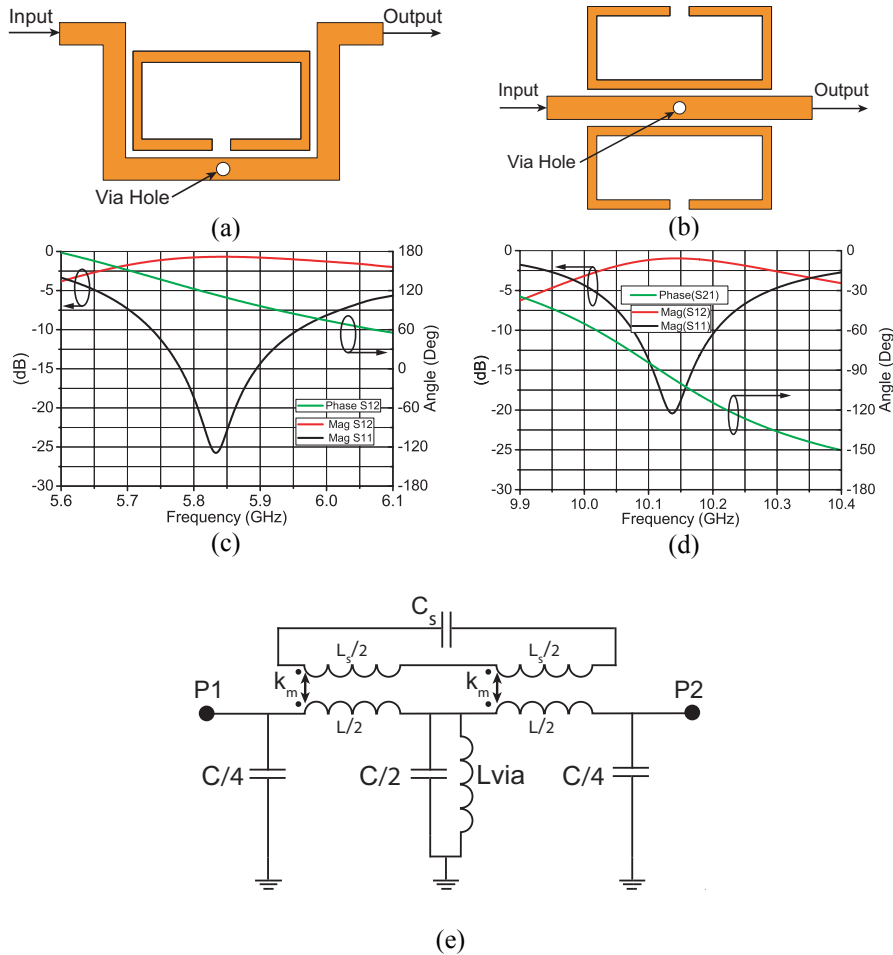


**Fig. 3** Phase shifters based on the *left-handed* unit cell: (a) SRRs coupled with meander line, (b) Two pairs of SRRs, (c)  $S$ -parameters for (a), (d);  $S$ -parameters for (b), (e) Equivalent circuit of the microstrip line loaded with SRRs and grounded with via.

In Fig. 3b shifter based on the four SRR *left-handed* cell is shown [24]. Two pairs of SRRs in balanced microstrip technology are coupled with a transmission line in a similar manner like the previous one. The obtained characteristics are scanning sector of  $30^\circ$  for 2.5% of the relative bandwidth, which requires a phase shift of  $\pm 47^\circ$  and required  $L$  would be  $10.35\lambda_0$ . In [24] Rogers 5880 is used, with the dielectric constant of 2.17, the height of 0.508 mm, loss tangent is 0.001. Surface roughness in Rogers 5880 is 0.3 microns and is

significantly smaller than the one in Rogers 4003C, which would mean that at the same frequency, losses in metal would be considerably larger for Rogers 4003C. In both cases impedance of the transmission line is  $100 \Omega$ , and losses in the transmission line are 0.058 dB/cm for Rogers 4003C at 6 GHz [23], and 0.035 dB/cm for Rogers 5880 at 10 GHz [24].

From these two examples, we can see a significant advantage in the application of different phase shifter structures for enhancing frequency-scanning characteristics of the antenna array. In Figs. 3c and 3d the  $S$ -parameters of the corresponding shifters are given. In Fig. 3e the equivalent circuit of the shifters is shown and it can be derived from [25]. Based on the characteristics it can be seen that these shifters exhibit the behavior of the pass-band filter, hence controlling its zeros and poles desired characteristics could be obtained.

## 2.4. Linear arrays with identical rectangular dipoles

### A. Scanning antenna array at 6 GHz

Previously discussed shifters are used in the antenna array design. Radiating elements are simple identical rectangular dipoles. One-half of the dipole is at the top layer (brown) and the other is at the bottom (yellow) Fig. 4c. The structure is designed in a balanced microstrip technology so in order to connect it to a standard SMA connector, a transition from the balance-to-unbalance line (balun) is necessary. This is achieved via the triangular balun. The shifter from Fig. 3a is used in the antenna design in [23]. From Fig. 4a we can see that the antenna array achieved the scanning sector from  $45^\circ$  to  $77^\circ$ , frequency sensitivity of  $10.67^\circ/100$  MHz and gain is from 12.4 to 13.73 dBi. Dimensions of the rectangular dipoles are calculated in order to be resonant at a specific frequency with specific resistance value ( $Z = 400 \Omega + 0j$ ). The position of the resonance is determined with the length of the dipole and value of the resistance is regulated with the dipole width. Since there are two variables and two goals it is more tuning than an optimization. For a true optimization it necessary to have a certain degree of freedom, that is to have more variables than goals, which is the case in the pentagonal dipoles.

### B. Scanning antenna array at 10 GHz

The shifter shown in Fig. 3b is implemented at a higher frequency of 10 GHz. The produced prototype is shown in Fig. 4e. The array is placed above the reflector plane at the distance  $D = 7.5$  mm. Dipoles are designed to have an impedance around  $400 \Omega$  at 10 GHz, with the distance between radiating dipoles of  $0.5\lambda_0$ , that is 15 mm at 10 GHz. In Fig. 4g we can see the offset between measured and simulated  $S_{11}$  parameter due to the fact that the SMA connector is not precisely modeled and interconnection between the structure of the balun and the connector can produce discrepancy. Nevertheless, the measured  $S_{11}$ -parameter exhibits a good matching in the working bandwidth from 10 to 10.3 GHz. From Fig. 4b we can again see a slight offset between the measured and simulated radiation characteristics due to manufacturing imperfections. Measured characteristics show scanning from  $105^\circ$  to  $130^\circ$ , gain variation from 12.1 to 12.9 dBi and frequency sensitivity of  $8.33^\circ/100$  MHz. As can be seen, these two shifters are designed to produce the frequency scanning at the different angles and scan rates, but both antenna arrays in this configurations display very high SLLs since the identical radiating elements are used in the array. In the first case, SLLs are from -10 dB to -7.5 dB below the main beam while in the second case their measured values are from -11.5 to -9 dB below the main beam. The high SLLs are usually the biggest issues with scanning antennas.

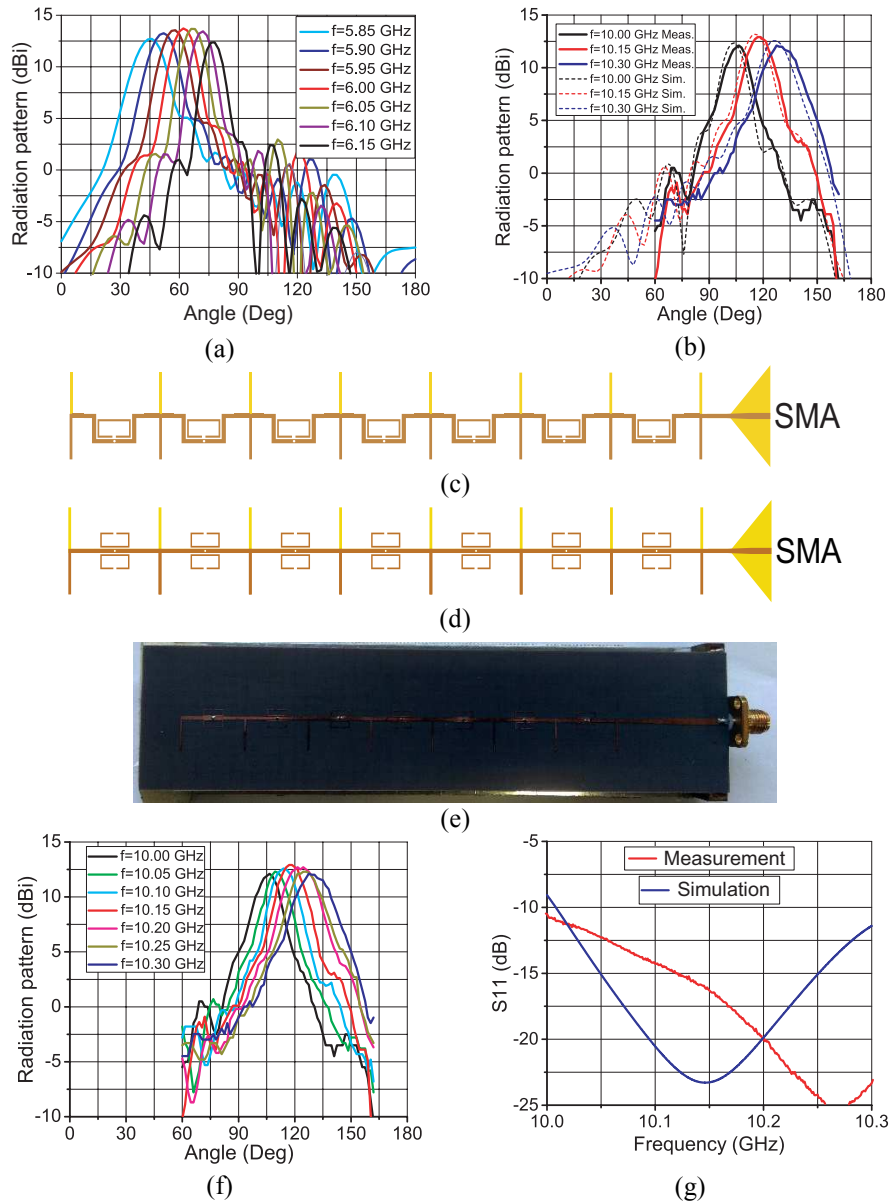


**Fig. 4** Comparison of the antenna arrays with different phase shifters operating at 6 GHz and 10 GHz: (a) Simulated radiation pattern for the antenna array with phase shifter shown in Fig. 3a, (b) Simulated and measured radiation pattern for the antenna array with phase shifter shown in Fig. 3b at the central and edge frequencies, (c) Model of the antenna array with shifter shown in Fig. 3a, (d) Model of the antenna array with shifter shown in Fig. 3b, (e) Antenna prototype with dimensions 146.2 mm x 35.75 mm, (f) Measured radiation pattern, (g) Measured and simulated  $S$ -parameters of the array from Fig. 4e.

## 2.5. Linear array with pentagonal dipoles

In order to obtain a higher side lobe suppression in the antenna array, the appropriate power distribution is necessary to be implemented. This problem is particularly challenging in the case of the linear scanning array with series feeding. The typical configuration of the traveling wave antenna array employs radiating elements of different impedances, so when wave travel through the array each radiating element takes the portion of the power available, which depends on its impedance value. At the end of the array, there is a termination for preventing the remaining power to return to the array and cause additional scanning beam in the opposite direction in relation to the broadside. Shifters can have significant losses, which can considerably degrade the radiation characteristics. Its influence on the power distribution must be seriously considered.

Another important issue is the fact that frequency scanning means that the antenna operates in a certain frequency band. The elements of the antenna array are frequency dependent and have different behavior depending on the observing frequency. Power distribution is mostly implemented based on the ratio of the impedances of the transmission line and the radiation elements. An approach that is more proper would be observing  $S$ -parameters on the multi-port network thus directly observe power distribution in the frequency range. In order to preserve power distribution in the frequency range, all components should have slow impedance change, which would result in stable  $S$ -parameters. This can be accomplished using pentagonal printed dipoles as radiating elements and shifter from Fig. 3. Approximation of the impedance values for the specific distribution can be calculated by:

$$Z_j = 10^{10} \frac{a_j Z_{norm}}{(w_j(n,k))^2} \quad (2)$$

where  $Z_j$  represents the impedance in Ohms of the  $j^{th}$  element of the array, where  $j = 1..n$  and  $n$  is the number of the elements of the array;  $a_j$  represents accumulated losses in the array at the  $j^{th}$  element, which mostly originated from the phase shifters and radiating losses;  $Z_{norm}$  is the constant impedance which value depends on the scope of value of the minimum and maximum available as the impedance of the radiating elements;  $w_j(n,k)$  is the weighting coefficient for the specific distribution for the case of the  $n$  elements and for  $k$  as a level of sidelobe suppression in dB. Implementation of this approach in the array with *right-handed* shifters is shown in [26]. For Dolph-Chebyshev distribution with  $n = 8$  and  $k = 21$ ,  $a_j = 1.5(j-1)$  impedance values are given in Table 1.

**Table 1** Impedance values for the array with the pentagonal dipoles.

| $Z_1$  | $Z_2$ | $Z_3$ | $Z_4$ | $Z_5$ | $Z_6$ | $Z_7$ | $Z_8$ |
|--------|-------|-------|-------|-------|-------|-------|-------|
| 1570.8 | 750.2 | 292.3 | 156.1 | 110.5 | 103.7 | 133.4 | 140   |

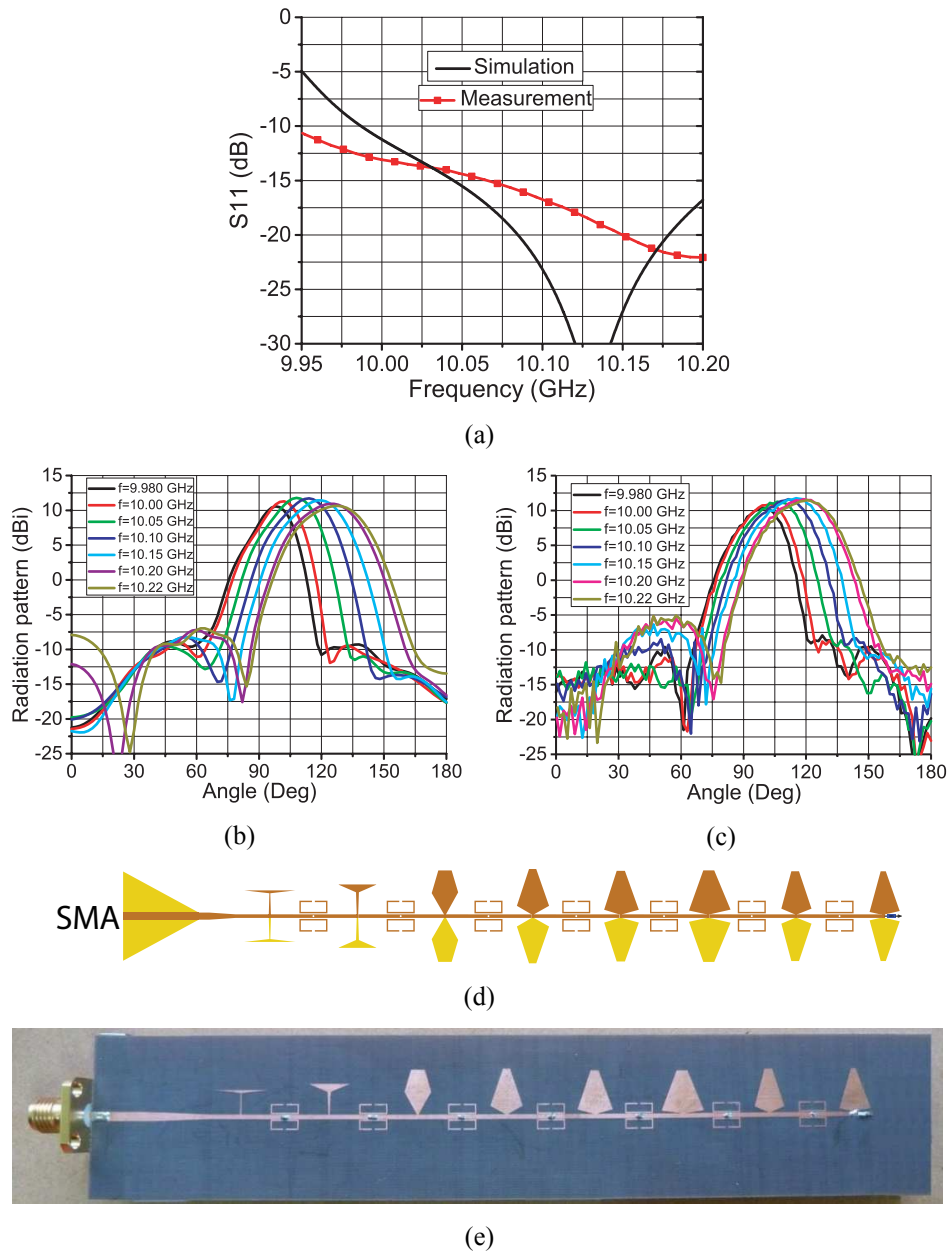


**Fig. 5** (a) Measured and simulated  $S$ -parameters of the linear array with pentagonal dipoles, (b) Simulated radiation pattern, (c) Measured radiation pattern, (d) Model of the array, (e) Manufactured prototype with dimensions: 140 mm x 27 mm.

Measured and simulated  $S$ -parameters are shown in Fig. 5a. The measured  $S_{11}$  characteristic is better than simulated one due to the additional losses. Simulated and measured radiation characteristics are shown in Figs. 5b and 5c, respectively. The power distribution used in the array is Dolph-Chebyshev, with the goal to achieve SLLs suppression of 20 dB in respect to the level of the main beam. In Fig. 5b we can see that the goal is achieved and in the whole range SLLs are below desired level. The measured results show some degradation due to manufacturing errors and slightly lower gain due to losses. The model and manufactured prototype are shown in Figs. 5d and 5e, respectively.

The detailed comparison of the manufactured antennas characteristics are shown in Table 2. From it, we can see that using pentagonal dipoles with different impedances, the main problem with printed scanning arrays can be resolved. The great improvement in SLLs is achieved. The trade-off of SLLs improvement is a wider 3 dB beamwidth and somewhat lower antenna gain.

**Table 2** Comparison of the measured characteristics of the antenna arrays with identical rectangular and different pentagonal dipoles.

| Dipoles               | Rectangular               | Pentagonal               |
|-----------------------|---------------------------|--------------------------|
| Bandwidth             | 10.00 GHz-10.30 GHz       | 9.98 GHz-10.22 GHz       |
| Scanning angle        | 100°-125° (25°)           | 100°-122° (22°)          |
| Frequency sensitivity | 83.333°/GHz               | 91.666°/GHz              |
| 3 dB beamwidth        | 14.26° – 22.6°            | 21.2°-29.2°              |
| Gain                  | 12.1 dB – 12.9 dB         | 10.4 dB - 11.7 dB        |
| SLL                   | <b>Better than 7.5 dB</b> | <b>Better than 17 dB</b> |

Measurements were performed using Anritsu ME7838A vector network analyzer [27] in a setup which consists of the calibration kit, two identical standard horn antennas, device under test (DUT), cables, positioner with stepper motor and PC control via Arduino MEGA 2560 motherboard [28]. Software communication with Arduino is done with Matlab through MATLAB Support Package for Arduino hardware [29]. At the same time software communication with Anritsu ME7838A, is done with Instrument Control Toolbox through LAN using TCP/IP [30]. One horn antenna is used as a transmitting antenna during the whole measurement procedure and the second one is used only at the beginning to determine relative gain levels at the position of the DUT. After placing DUT at the positioner with stepper motor the whole process is done automatically. Accuracy should be better than 0.5 dB.

### 3. CONCLUSION

In this paper, we have shown the use of the phased shifters based on the metamaterials. Shifters are analyzed and their performance is discussed. Their use in the frequency scanning arrays is shown. Two prototypes are produced and shown. It is demonstrated that a combination of the pentagonal dipoles with different impedances and metamaterial based shifters can provide frequency scanning and SLLs control thus making it a good choice for cheap and highly accurate frequency scanning solution.

**Acknowledgement:** This work was financed by the Serbian Ministry for Education, Science and Technological Development through the projects TR-32024 and III-45016. The authors would like to thank the Institute IMTEL, Belgrade, for the prototype manufacturing and to WIPL-D, Belgrade for the use of software licenses.

#### REFERENCES

- [1] M. Miljić, A. Nešić, B. Milovanović, "An investigation of side lobe suppression in integrated printed antenna structures with 3D reflectors", *Facta Universitatis, Series: Electronics and Energetics*, vol. 30, no. 3, pp. 391–402, September 2017.
- [2] C. Balanis, *Antenna Theory: Analysis and Design, 3rd ed.* Hoboken, New Jersey, United States, John Wiley, 2005.
- [3] T. A. Miligan, *Modern Antenna Design, 2nd ed.* Hoboken, New Jersey, United States, John Wiley, 2005.
- [4] W.S.T. Rowe and R. B. Waterhouse, "Edge-fed patch antennas with reduced spurious radiation", *IEEE Trans. Antennas Propag.*, vol. 53, no. 5, pp.1785–1790, May 2005.
- [5] J. L. Volakis, *Antenna Engineering Handbook, 4th ed.* New York, United States, McGraw-Hill Education, 2007.
- [6] D. F. Sievenpiper, L. Zhang, R. F. Jimenez Broas, N. G. Alexópoulos, and E. Yablonovitch, "High-impedance electromagnetic surfaces with a forbidden frequency band," *IEEE Trans. Microwave Theory Tech.*, vol. 47, no. 11, pp. 2059–2074, Nov. 1999.
- [7] C. S. Lee, V. Nalbandian, and F. Schwing, "Surface-mode suppression in a thick microstrip antenna by parasitic elements," *Microwave and Opt. Technol. Lett.*, vol. 8, pp. 145–147, Feb. 1995.
- [8] N. G. Alexopoulos and D. R. Jackson, "Fundamental superstrate (cover) effects on printed circuit antennas," *IEEE Trans. Antennas Propag.*, vol. 32, no. 8, pp. 807–816, Aug. 1984.
- [9] D. R. Jackson, J. T. Williams, A. K. Bhattacharyya, R. L. Smith, S. J. Buchheit, and S. A. Long, "Microstrip patch designs that do not excite surface waves," *IEEE Trans. Antennas Propag.*, vol. 41, no. 8, pp. 1026–1037, Aug. 1993.
- [10] Komanduri, V.R., Jackson, D.R., Williams, J.T., and Mehrotra, A.R.: "A general method for designing reduced surface wave microstrip antennas", *IEEE Trans. Antennas Propag.*, vol. 61, no. 6, pp. 2887–2894, March 2013.
- [11] R. J. Mailloux, *Phased Array Antenna Handbook, 2nd ed.* London: Artech House antennas and propagation library, 2005.
- [12] M. Winfried, M. Wetzel and M. Menzel, "A novel direct imaging radar sensor with frequency scanned antenna," *In Proceedings of the IEEE MTT-S Int. Microwave Symp. Dig.*, 2003, vol. 3, pp.1941–1944.
- [13] Y. Alvarez Lopez, C. Garcia, C. Vazquez, S. Ver-Hoeve, and F. Las-Heras, "Frequency scanning based radar system," *Prog. Electromagn. Res.* vol. 132, pp. 275–296, 2012.
- [14] Alvarez, Y., Cambior, R., Garcia, C., et al.: "Submillimeter-wave frequency scanning system for imaging applications", *IEEE Trans. Antennas Propag.*, vol. 61, no 11, pp. 5689–5696, Nov. 2013.
- [15] M. A. Tehrani, J. J. Laurin, and Y. Savaria, "Multiple targets direction-of-arrival estimation in frequency scanning array antennas," *IET Radar, Sonar and Navigation*, vol. 10, no. 3, pp. 624–631, March 2016.
- [16] S. Vashist, M. K. Soni and P.K. Singhal, "A Review on the Development of Rotman Lens Antenna", *Chinese Journal of Engineering*, vol. 2014, Article ID 385385, 9 pages, 2014.
- [17] W. Zongxin, X. Bo and Y. Fei, "A Multibeam Antenna Array Based on Printed Rotman Lens", *International Journal of Antennas and Propagation*, vol. 2013, Article ID 179327, 6 pages, 2013.
- [18] J. Remez ; R. Carmon, "Compact Designs of Waveguide Butler Matrices", *IEEE Antennas Wireless Propag. Lett.*, vol. 5, pp. 27–31, March 2006.
- [19] M. Koubeissi, L. Freytag, C. Decroze, and T. Monediere, "Design of a cosecant-squared pattern antenna fed by a new Butler matrix topology for base station at 42 GHz," *IEEE Antennas Wireless Propag. Lett.*, vol. 7, pp. 354–357, 2008.
- [20] M. Ilić i N. Bošković, "Poređenje karakteristika štampanih bow-tie dipola sa dipolima petougaoonog oblika", In Proceedings of the ETRAN Conference 2012, Zlatibor, 11-14. jun 2012.
- [21] A. Nešić, Z. Mičić, S. Jovanović, I. Radnović, D. Nešić, "Millimeter-Wave Printed Antenna Arrays for Covering Various Sector Widths", *IEEE Antennas and Propagation Magazine*, vol. 49, no. 1, pp. 113–118, February 2007.
- [22] <https://www.itu.int/>

- [23] N. Bošković, B. Jokanović i A. Nesić, "Frekvencijski skeniran antenski niz sa SRR faznim šifterima", In Proceedings of the ETRAN Conference 2013, Zlatibor, 3-6. jun 2013.
- [24] N. Boskovic, B. Jokanovic and A. Nestic, "Frequency Scanning Antenna Array with Enhanced Side lobe Suppression", *Metamaterials 2014*, Copenhagen, Denmark, 25-30. August 2014.
- [25] R. Bojanic, V. Milosevic, B. Jokanovic, F. Medina-Mena and F. Mesa, "Enhanced Modelling of Split-Ring Resonators Couplings in Printed Circuits," *IEEE Trans. Microw. Theory Tech.*, vol. 62, no. 8, pp. 1605–1615, 2014.
- [26] N. Boskovic, B. Jokanovic, and M. Radovanovic, "Printed frequency scanning antenna arrays with enhanced frequency sensitivity and sidelobe suppression," *IEEE Trans. Antennas Propag.*, vol. 65, no. 4, pp. 1757–1764, Apr. 2017.
- [27] "Installation Guide VectorStar ME7838 Series." <https://dl.cdn-anritsu.com/en-us/test-measurement/files/Manuals/Installation-Guide/10410-00293F.pdf>
- [28] "Arduino Mega 2560 Rev3." <https://store.arduino.cc/arduino-mega-2560-rev3>
- [29] "MATLAB Support Package for Arduino Hardware Documentation." <https://www.mathworks.com/help/supportpkg/arduinoio/index.html>
- [30] "Instrument Control Toolbox." <https://www.mathworks.com/products/instrument.html>